Sensors **2010**, *10*, 3057-3072; doi:10.3390/s100403057

OPEN ACCESS

sensors

ISSN 1424-8220

www.mdpi.com/journal/sensors

Article

The Assessment for Sensitivity of a NO_2 Gas Sensor with $ZnGa_2O_4$/ZnO Core-Shell Nanowires—a Novel Approach

I-Cherng Chen [1,*], Shiu-Shiung Lin [2], Tsao-Jen Lin [3], Cheng-Liang Hsu [4], Ting Jen Hsueh [5] and Tien-Yu Shieh [2,*]

[1] Micro Systems Technology Center, ITRI South, Industrial Technology Research Institute, Tainan 709, Taiwan

[2] College of Dental Medicine, Kaohsiung Medical University, Kaohsiung 807, Taiwan

[3] Chemical Engineering Department, National Chung-Cheng University, Chia-Yi, 621, Taiwan

[4] Department of Electronic Engineering National University of Tainan, Tainan, 700, Taiwan

[5] National Nano Device Laboratories, Tainan 741, Taiwan

* Authors to whom correspondence should be addressed; E-Mails: eugenechen@itri.org.tw (I-C.C.); tiyush@kmu.edu.tw (T.-Y.S.).

Received: 15 March 2010; in revised form: 23 March 2010 / Accepted: 24 March 2010 / Published: 30 March 2010

Abstract: The application of novel core-shell nanowires composed of $ZnGa_2O_4$/ZnO to improve the sensitivity of NO_2 gas sensors is demonstrated in this study. The growth of $ZnGa_2O_4$/ZnO core-shell nanowires is performed by reactive evaporation on patterned ZnO:Ga/SiO_2/Si templates at 600 °C. This is to form the homogeneous structure of the sensors investigated in this report to assess their sensitivity in terms of NO_2 detection. These novel NO_2 gas sensors were evaluated at working temperatures of 25 °C and at 250 °C, respectively. The result reveals the $ZnGa_2O_4$/ZnO core-shell nanowires present a good linear relationship ($R^2 > 0.99$) between sensitivity and NO_2 concentration at both working temperatures. These core-shell nanowire sensors also possess the highest response (<90 s) and recovery (<120 s) values with greater repeatability seen for NO_2 sensors at room temperature, unlike traditional sensors that only work effectively at much higher temperatures. The data in this study indicates the newly-developed $ZnGa_2O_4$/ZnO core-shell nanowire based sensors are highly promising for industrial applications.

Keywords: $ZnGa_2O_4$; ZnO; core shell; nanowire; NO_2; gas sensor; sensitivity

1. Introduction

Nitrogen dioxide (NO_2) is a toxic compound with a pungent odor that is harmful to the environment as a major cause of acid rain and photochemical smog. NO_2 is mainly produced by power plants, combustion engines and automobiles. It can also be noxious and induce health problems, such as olfactory paralysis. Safety guidelines recommend that humans should not be exposed to more than 3 ppm NO_2 gas for periods longer than 8 hours [1-3]. Therefore, it is highly desirable to develop a reliable sensor that can effectively detect NO_2 even with extremely low concentration.

An ideal sensor can be utilized in an early warning system for environmental monitoring to detect the presence of NO_2 before a critical condition occurs. The demand to produce ideal NO_2 sensors has propelled considerable research activities in the relevant fields. Various types of metal oxide based sensors composed of TiO_2, SnO_2, ZnO, or WO_3 have been used extensively to detect toxic and pollutant gases, such as NO_x, H_2S, Cl_2, CO, SO_2, and O_3. Other combustible gases, including H_2, CH_4 and flammable organic vapors are also detectable by these compound based sensors [4-6]. Recently, numerous compounds have been applied for NO_2 detection, and YSZ, NASICON, ZnO, In_2O_3, and WO_3 have been extensively investigated [7-19]. Among them, ZnO is a chemically and thermally stable n-type semiconductor which is highly advantageous for the development of the ideal sensors. It incorporates both massive exciton binding energy (60 MeV) and significant band-gap energy (3.37 eV) at room temperature [20]. ZnO subsequently is frequently applied for generating novel detectors, particularly for NO_2 [21]. ZnO gas sensors were widely demonstrated in the forms of thick films, thin films, heterojunctions, nanoparticles, and nanowires [10,11,22-28]. It is also noted that the use of semiconductor metal oxide materials for gas sensing generally involves some chemical reaction with gas molecules on the oxide surface [29].

Nowadays one-dimensional ZnO nanowires are drawing considerable attention for their larger surface-to-volume ratio than bulk ZnO and ZnO films [30]. Due to its larger surface area, the nanowire-based gas sensors tend to provide much higher sensitivity. Laboratory manipulations and manufacture of ZnO nanowires have been reported in our previous studies. These include vertical growth of ZnO nanowires on various substrates without catalyst [31-34], introduction of dopants into the ZnO nanowires [35,36], and production of vertical core–shell nanowires grown of $ZnGa_2O_4$/ZnO by applying a low-pressure chemical vapor transport [37,38]

$ZnGa_2O_4$ is an attractive low-voltage phosphor [39,40]. It is a transparent conducting oxide with a wide band-gap and a spinel crystal structure [41,42]. The structure of $ZnGa_2O_4$/ZnO core-shell nanowires uniquely consists of a ZnO core and a thin layer of spinel $ZnGa_2O_4$ shell. Its use in gas sensors has not been formally reported, despite its advantageous characteristics. It is well known that spinel oxides (AB_2O_4) can be used as gas sensor materials because of their stability to thermal and chemical conditions.

It is proposed in this study to apply $ZnGa_2O_4$/ZnO core-shell nanowires as a novel sensor for NO_2 detection. It is generated on patterned ZnO:Ga/SiO_2/Si templates at 600 °C by reactive evaporation to form a form simple sensing structure. This research reports the manufacturing procedures and its chemical sensing properties for NO_2 tracing. The potential industrial application of $ZnGa_2O_4$/ZnO core-shell nanowires is also discussed.

2. Materials and Methods

2.1. Preparation of Chemicals and Materials

p-Type (100) oriented Si wafers (Si Wave Co., Taiwan) were used as the substrates. They were initially cleaned by an RCA standard process to remove organic contaminants, and then rinsed under running de-ionized water. To thoroughly remove native oxide, the wafers were dipped into 48% HF solution for 10 seconds, and flushed by dry nitrogen. The chemicals used in this study included Zn metal powder (99.9%, 300 mesh, Strem Chemicals, Newburyport, MA, USA), Gallium powder (99.99%, 100 mesh, American Elements Products), O_2 (99.999%, Air Products, Taiwan), N_2 (99.99%, Air Products, Taiwan) and Ar (99.999%, Air Products, Taiwan). The target of ZnO:Ga with a mixture of ZnO (99.99% Strem Chemicals) and Ga_2O_3 (99.999%, Strem Chemicals) was employed as source materials. The target was prepared using conventional sintering process. The amount of Ga_2O_3 added to the target was 3 wt%. All aqueous solutions were prepared with purified water obtained from the Ropure ST water purification system (Barnstead) with a specific resistance of 18 Mohm-cm.

2.2. Preparation of $ZnGa_2O_4$/ZnO Core-Shell Nanowire Based Sensors

Figure 1 schematically depicts the growth and processing steps used in this study. Prior to growing the $ZnGa_2O_4$/ZnO core-shell nanowires, a cleaned Si (100) substrate was thermally oxidized to form a 500 nm-thick SiO_2 film. A 100 nm-thick Ga-doped ZnO thin film was subsequently deposited onto the SiO_2 film by RF magnetron sputtering. X-ray diffraction (XRD) measurement showed that the sputtered ZnO:Ga film was oriented along the (0 0 2) direction. The sheet resistance of the sputtered ZnO:Ga film was evaluated by four-point resistivity measurement, and it was found to be around 200 Ω/sq. Afterwards, a comb-like pattern was formed by partially etching away the ZnO:Ga film with standard photolithography methods. During wet etching, the template was dipped in 2% HCl for 3 min to remove the exposed ZnO:Ga. Through the designed etching mask, the fingers of the comb-like pattern were developed in 10 μm wide and 80 μm long with a spacing of 10 μm, as shown in Figure 1. Subsequently, two small pieces of glasses were used to cover the two electrodes of the patterned ZnO:Ga film to prevent growing $ZnGa_2O_4$/ZnO core-shell nanowires in these regions.

To grow the $ZnGa_2O_4$/ZnO core-shell nanowires, the patterned ZnO:Ga/SiO_2/Si substrate and Zn/Ga mixture powder were placed in an alumina boat, and then the alumina boat inserted into a quartz tube. Zinc metal powder with 99.9% purity was applied as the Zn source, and the Ga source was 99.99% pure Ga powder. Before growth, Zn and Ga ingredients were prepared by grinding these powders together into fine mixtures with ratio of 0.3 g/0.15 g.

Constant streams of argon (54.4 sccm) and oxygen (0.8 sccm) gases were then introduced into the furnace. The critical positions and processing temperature of the patterned ZnO:Ga/SiO_2/Si substrate, Zn/Ga vapor source and alumina boat were carefully controlled. They have to be located at the same horizontal level and heated at the same temperature. A mechanical pump was subsequently employed to evacuate the system, and a programmable temperature controller was used to precisely control the furnace temperature with an accuracy of ±1 °C. During the growth of nanowires, the quartz tube pressure and the growth temperature were maintained at 10 Torr and 600 °C, respectively. The process

lasted 60 minutes. For comparison purposes, pure ZnO nanowires without any Ga were also prepared under exactly the same conditions.

Figure 1. The growth and processing steps of $ZnGa_2O_4$/ZnO core-shell nanowire based sensors.

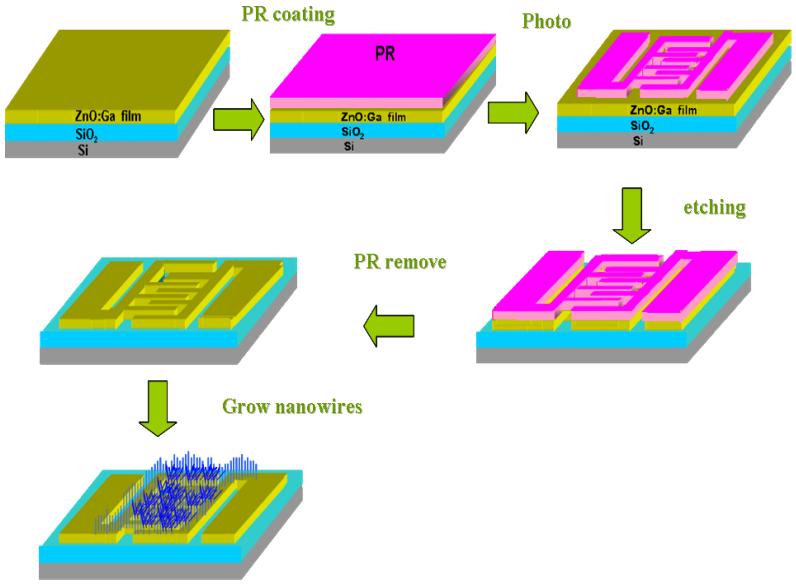

2.3. Characterization of $ZnGa_2O_4$/ZnO Core-Shell Nanowires

A MAC MXP18 X-ray diffractometer and a JEOL JEM-2100F high resolution transmission electron microscopy (HRTEM), operated at 200 KV, were then used to characterize the crystallography and structure of the as-grown nanowires. The surface morphologies of the samples and the size distribution of the nanowires were characterized using a JEOL JSM-6500F field emission scanning electron microscope (FESEM), operated at 5 KeV. Photoluminescence (PL) properties of the as-grown ZnO nanowires were also characterized by a Jobin Yvon-Spex fluorolog-3 spectrophotometer. A Xe lamp emitting at 254 nm was applied as the excitation source during PL measurements.

2.4. Measurement of Gas Sensing Properties

To measure gas sensing properties of the nanowires, the sample was prepared in a sealed glass chamber. Its resistivity in air was measured from the two electrodes of the patterned ZnO:Ga film. In this study, NO_2 gas was used as the target for detection. NO_2 gas was carried by air or N_2 into the glass chamber through a mixer. Gas-sensing tests were all performed at room temperature. The total flow rate of the NO_2 and the carrier gas was kept constantly at 100 cm^3/min in each test. In order to control temperature, a small heater equipped with a thermocouple was used. The screen printing method was utilized to produce the heating plate, by using the RuO_2 paste on alumina substrate with silver-printed electrodes (area: 10 mm × 10 mm; heater resistance: 30 ohm). Manipulation of NO_2 concentrations was carried out by modulating the ratio of the flow rate of NO_2 gas to that of the carrier gas. The

electrical response of the sensor was measured with a computer-loaded analytic system. A voltage detecting method was used to calculate the sensitivity of the sensor, and it was defined as:

$$S = (R_s - R_{air}) / R_{air} \quad (1)$$

where S represents sensitivity, R_s and R_{air} were the electrical resistances in NO_2 and synthetic air, respectively. To observe dynamic and repetitive responses, the sensor was fixed on a temperature-controlled heater, and placed inside a 100-mL glass chamber. The testing gas mixture was continuously flowing into the glass chamber. The flow rate was kept constantly at 100 cm^3/min, and NO_2 concentrations in synthetic air were varied from 1–100 ppm. Pure ZnO nanowires without any Ga were also prepared and tested in the same way as the control group.

3. Results and Discussion

3.1. Morphological and Electronic Properties of $ZnGa_2O_4$/ZnO Core-Shell Nanowires

Figure 2 shows the schematic illustration for a cross network of $ZnGa_2O_4$/ZnO core-shell nanowires floating on a patterned ZnO:Ga/SiO_2/Si substrate. The structure of $ZnGa_2O_4$/ZnO core-shell nanowires consists of a ZnO core and a thin layer of $ZnGa_2O_4$ shell. These grow on conductive film of ZnO:Ga in the vertical and orderly shape, compared with cross network structure of growth on SiO_2 insulation of spacer regions, which constitutes a simple gas sensor. A simple and efficient way is presented in this study to produce the $ZnGa_2O_4$/ZnO core-shell based gas sensors with self-assembly. This process is inexpensive and feasible for nano-devices, and it is illustrated as below:

Figure 2. A schematic diagram of cross network structure as sensing layers of the $ZnGa_2O_4$/ZnO core-shell nanowires based sensors.

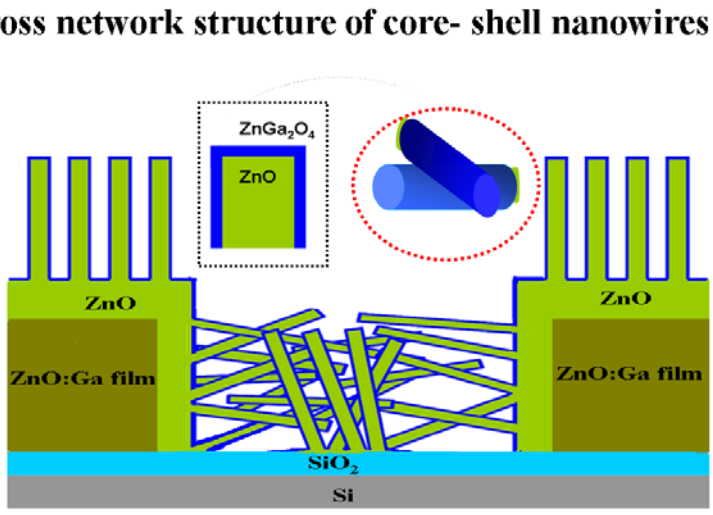

Figure 3(a) shows a top view FESEM image of the as-grown $ZnGa_2O_4$/ZnO core-shell nanowires prepared on the patterned ZnO:Ga/SiO_2/Si template. It was found that the $ZnGa_2O_4$/ZnO nanowires were grown vertically on the conducting ZnO:Ga finger regions. This should be attributed to the fact that these $ZnGa_2O_4$/ZnO core-shell nanowires were grown along the columnar grains of the underneath sputtered ZnO:Ga film [43]. In contrast, the growing alignment of $ZnGa_2O_4$/ZnO core-shell nanowires

grown on SiO_2 spacer regions in the inset of Figure 3(b) was randomly oriented. These randomly aligned $ZnGa_2O_4$/ZnO core-shell nanowires tend to provide electrical paths between the adjacent fingers. Figure 3(c) indicates the titled cross sectional FESEM images of the $ZnGa_2O_4$/ZnO core-shell nanowires vertical grown on the ZnO:Ga film regions the sample. Figure 3(d) demonstrated the X-ray diffraction (XRD) spectrum of the pure ZnO nanowires (*a-blue*-line) and the $ZnGa_2O_4$/ZnO core-shell nanowires (*b-red*-line), and this was prepared to characterize the structural properties.) In addition to ZnO-related peaks, the XRD spectrum in Figure 3(d) demonstrated $ZnGa_2O_4$ (111), (222), (511) and (444) peaks. This observation reveals that the nanowires possess a $ZnGa_2O_4$ crystal structure. The analysis of FESEM images show that the as-grown $ZnGa_2O_4$/ZnO nanowires present a core-shell structure with 0.8–5 μm in length and 40–100 nm in width. These core-shell nanowires, consisting of a ZnO core and a thin layer of spinel $ZnGa_2O_4$ shell, have not been investigated in terms of its efficacy of gas detection. It is therefore proposed to thoroughly inspect its NO_2 gas sensing mechanisms.

Figure 3. (a) FESEM image of $ZnGa_2O_4$/ZnO core-shell nanowires grown on patterned ZnO:Ga/SiO_2/Si substrate. (b) Enlarged SEM photographs of $ZnGa_2O_4$/ZnO core-shell nanowires grown on the SiO_2 spacer regions (c) Tilted cross sectional FESEM images of $ZnGa_2O_4$/ZnO core-shell nanowires grown on the ZnO:Ga film regions the sample (d) XRD spectrum of pure ZnO nanowires (a-blue-line) and $ZnGa_2O_4$/ZnO core-shell nanowires (b-red-line) prepared in this study.

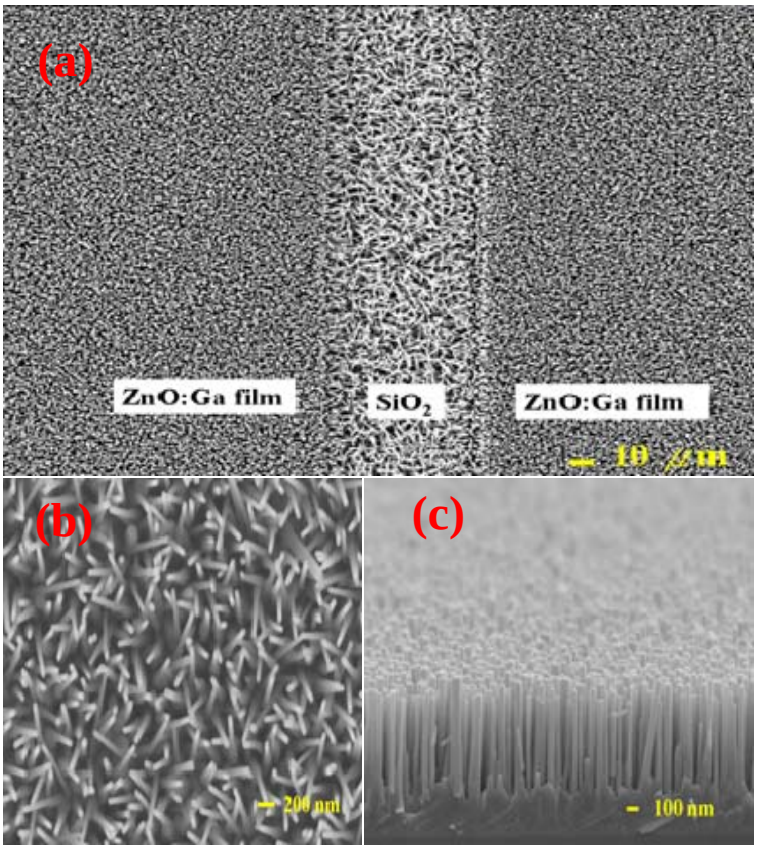

Figure 3. *Cont.*

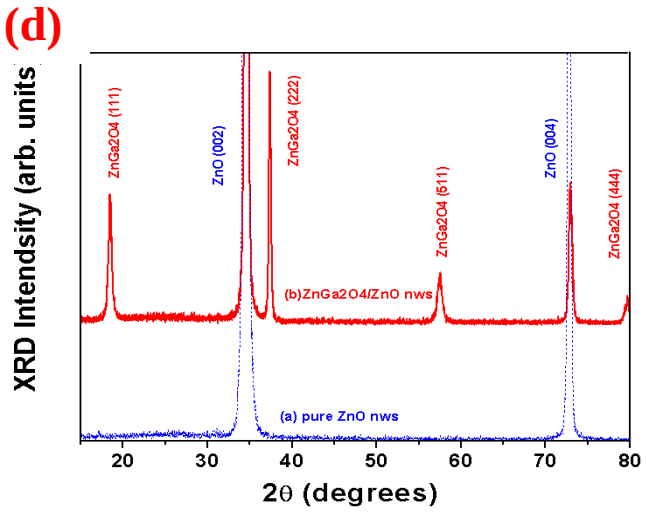

3.2. Efficacy and Sensitivity of Gas Detection of ZnGa2O4/ZnO Nanowires

For NO_2 gas sensing, oxygen sorption plays an important role in electrical transport properties of ZnO nanowires. The oxygen ionosorption removes conduction electrons and thus lowers the conductance of ZnO [44]. The reactive oxygen species such as O_2^-, O^{2-} and O^- are first adsorbed on ZnO surface when temperature rises. It is well known that the response of chemisorbed oxygen species strongly depends on temperature. At low temperatures, O_2^- is commonly chemisorbed. At high temperatures, however, O^- and O^{2-} are chemisorbed while O_2^- disappears [45]. The reaction kinematics can be described as follows [44]:

$$O_{2\ (gas)} \leftrightarrow O_{2\ (ads)} \tag{2}$$

$$O_{2\ (ads)} + e^- \leftrightarrow O_2^- \tag{3}$$

$$O_2^- + e^- \leftrightarrow 2\ O^- \tag{4}$$

When the ZnO nanowires are exposed to NO_2 gas, NO_2 gas tends to react with the adsorbed O^- ions and directly accumulate on the surface of ZnO nanowires. And its reactions are shown as below [47,48]:

$$NO_{2\ (gas)} + e^- \longrightarrow NO_2^-{}_{(ads)} \tag{5}$$

$$NO_2^-{}_{(ads)} + O^-{}_{(ads)} + 2e^- \longrightarrow NO_{(gas)} + 2O^{2-}{}_{(ads)} \tag{6}$$

Subsequently, the concentration of electrons on the surface of ZnO nanowires arrays decreases and the resistance of ZnO layer will increase accordingly. The adsorption of O^- ions is an very interesting and critical phenomenon in metal-oxide gas sensor, because the O^- ions tend to assist the adsorbed NO_2^- ions in taking the electrons from the nanowires arrays. The dynamic responses of $ZnGa_2O_4$/ZnO core-shell nanowires sensors at 250 °C were tested with four different NO_2 concentrations at 1, 2.5, 5 and 10 ppm, respectively (Figure 4). The gas-input period of NO_2 gas was varied from 90 to 360 seconds.

A complete recovery was observed after the regeneration process in dry air. Since NO_2 gas does not generate any poisoning effects on the sensors, it is very likely that its total recovery is highly attainable. This investigation also reveals that the latent period between each response of gas detection at 250 °C was much longer than we expected to observe steady-state. It is therefore proposed to apply 360 s between each test in order to standardize the procedure of signal recorded.

The result shown in Figure 5 is the sensitivity of the $ZnGa_2O_4$/ZnO core-shell nanowires sensors in response to repetitive adsorption–desorption cycles. The stability and reproducibility of the NO_2 sensors at 250 °C were demonstrated with four different NO_2 concentrations in 1, 2, 5 and 10 ppm, respectively.

Figure 6 shows the relative response of the sensor is linearly proportional to NO_2 concentration ranged from 1 to 10 ppm at 250 °C. The sensitivity can be calculated from the slope as 2.327 ppm^{-1} and the quality of the curve fit as $R^2 = 0.9994$. There are many nanowire-to-nanowire junctions at the networking points of $ZnGa_2O_4$/ZnO core-shell nanowires based sensor. Thus, the enhanced sensitivity of the $ZnGa_2O_4$/ZnO core-shell nanowires can be attributed to the changes in the resistance of the gas sensors due to both a surface depletion region of each nanowire and the potential barrier height in the junction.

Figure 4. Dynamic responses of $ZnGa_2O_4$/ZnO core-shell nanowire sensor to different NO_2 concentrations of (a) 1 ppm, (b) 2.5 ppm, (c) 5 ppm, and (d) 10 ppm in synthetic air at 250 °C, respectively.

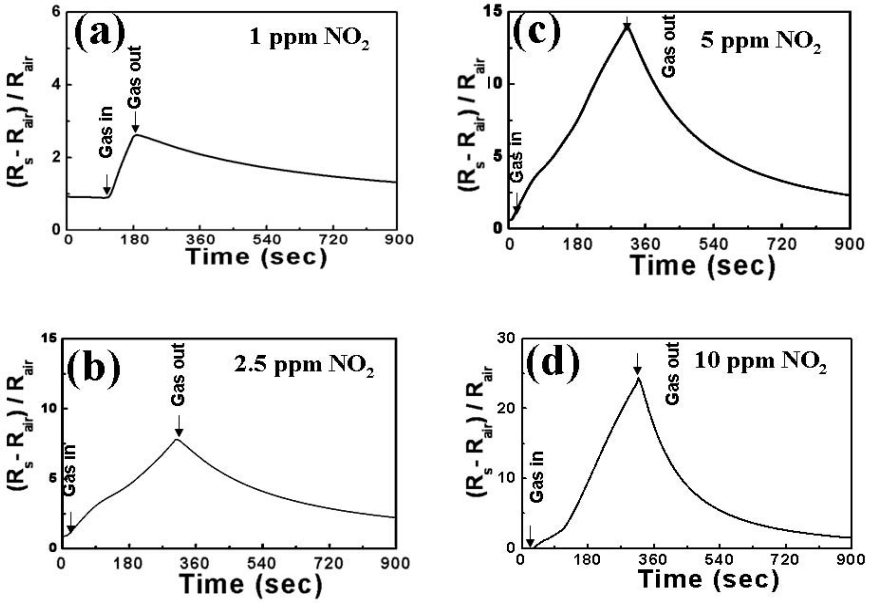

Figure 5. Repetitive response curves of $ZnGa_2O_4$/ZnO core-shell nanowires sensors operated at 250 °C. The different concentrations of testing gas are 1 ppm, 2.5 ppm, 5 ppm, and 10 ppm NO_2 in N_2 carrier gas.

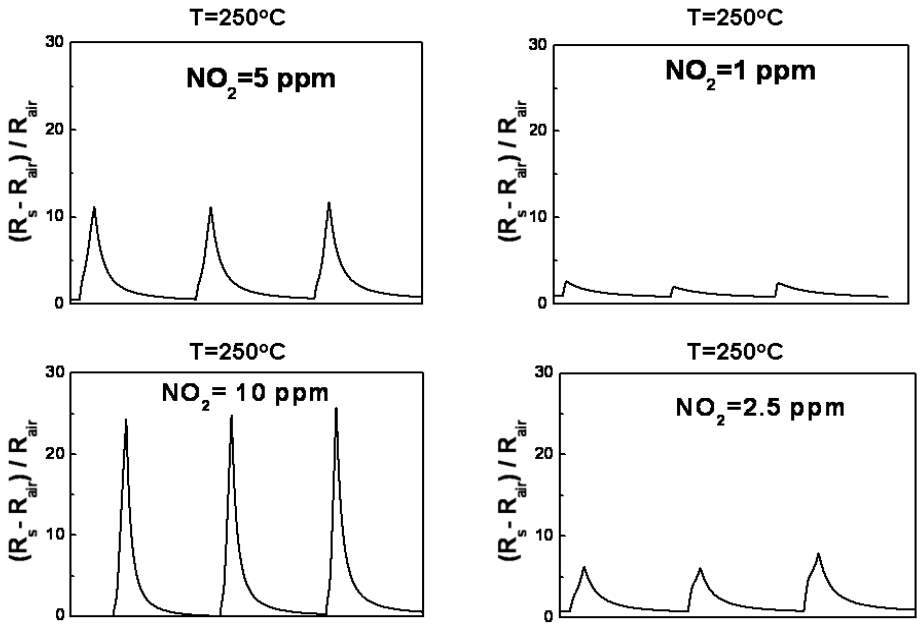

Figure 6. Response calibration of $ZnGa_2O_4$/ZnO core-shell nanowire sensors for different NO_2 concentrations at 250 °C.

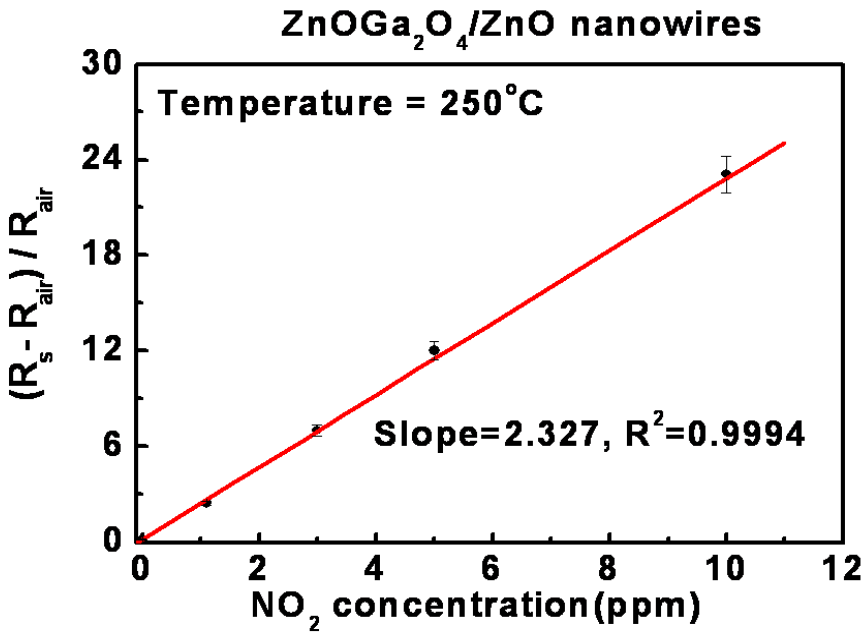

Figures 7 and 8 show the sensitivity of $ZnGa_2O_4$/ZnO core-shell nanowires sensor and ZnO nanowires sensor in response to repetitive adsorption–desorption cycles. The stability and reproducibility of the NO_2 sensor is demonstrated at 25 °C. The testing gas is 100 ppm NO_2 in N_2

carrier gas. The room temperature sensitivity observed here is most likely to be due to the high surface-to-volume ratio of the one-dimensional nanostructures. Meanwhile, since $ZnGa_2O_4$/ZnO core-shell nanowires are an n-type semiconductor, the oxidizing NO_2 molecules adsorbed on the oxide surface may capture electrons from the conduction band and form NO_2 [49]. This micro-property tends to increase the carrier concentration and leads to a greatly reduced resistivity of the nanowires. In our study [38], the electrical properties of $ZnGa_2O_4$/ZnO core-shell nanowires have been assessed by Hall-effect measurements in the previous study [39]. The outcome showed that the values of conductivity and carrier concentration are 33 S/cm and 1.02×10^{22} cm^{-3}, respectively. These are much higher than those of the pure ZnO nanowires (0.8 S/cm and 4×10^{16} cm^{-3}, respectively). The comparison of the data indicates the $ZnGa_2O_4$/ZnO core-shell nanowires are superior to ZnO nanowires in electric characteristics. The former is 40 times the conductivity, and the 2.55×10^5 times the carrier concentration of the latter. This explains the advantage of $ZnGa_2O_4$/ZnO core- shell nanowires for NO_2 sensing. Compared with the ZnO nanowires, the electric characteristic of $ZnGa_2O_4$/ZnO core-shell nanowires is 40 times higher on conductivity and 2.55×10^5 times higher on carrier concentration. For this reason we prefer using $ZnGa_2O_4$/ZnO core-shell nanowires for the NO_2 sensing.

Figure 7. Dynamic responses of $ZnGa_2O_4$/ZnO core shell nanowire sensor and ZnO nanowire sensor to 100 ppm NO_2 concentration in synthetic air at 25 °C.

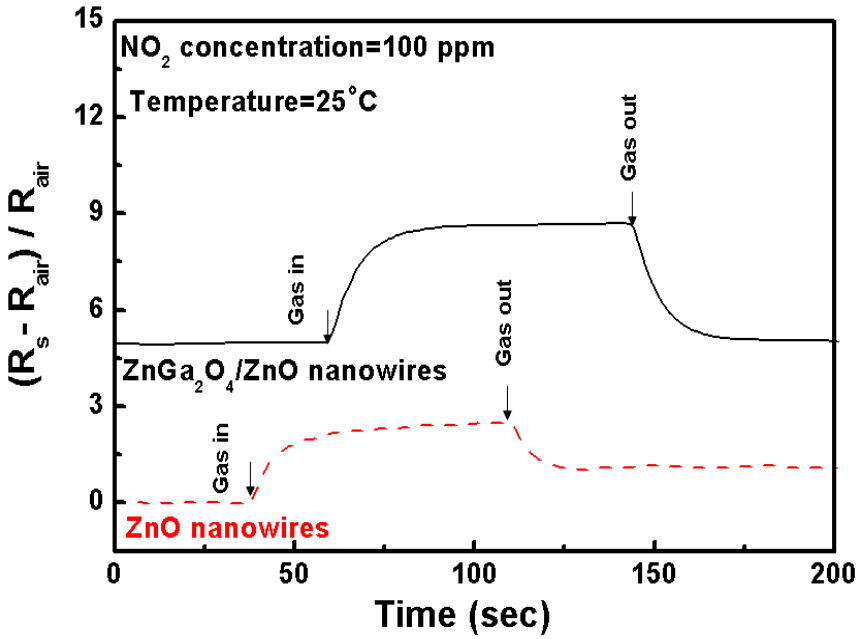

Figure 8. Repetitive response curves of $ZnGa_2O_4$/ZnO core-shell nanowire sensor and ZnO nanowire sensor at 25 °C, respectively. The testing gas is 100 ppm NO_2 in N_2 carrier gas.

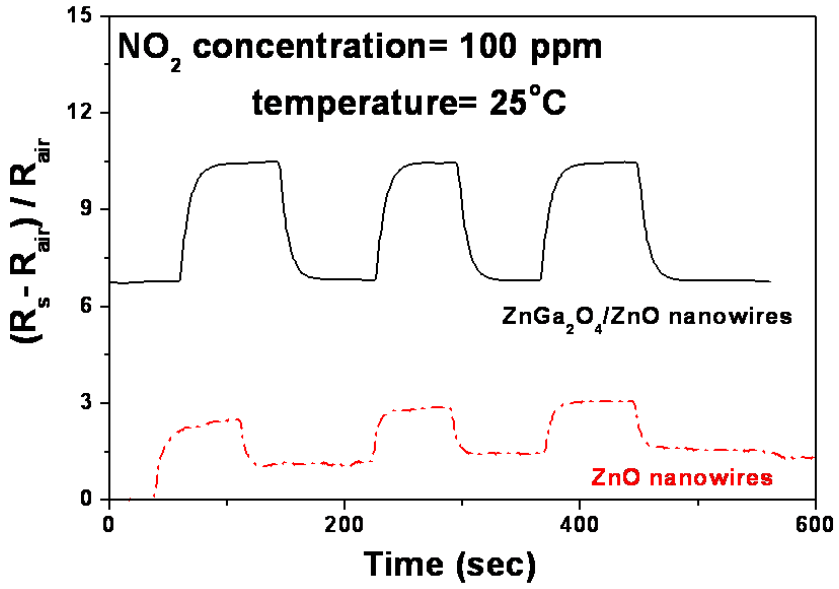

Figure 9 shows the relative response of the sensor is linearly proportional to different NO_2 concentrations ranged from 10 to 100 ppm at 25 °C. The sensitivity of $ZnGa_2O_4$/ZnO core-shell nanowire sensors calculated from the slope was 0.0494 ppm^{-1}, while the ZnO nanowire sensors only presents its sensitivity as 0.0223 ppm^{-1}.

Figure 9. Response calibrations of **(a)** $ZnGa_2O_4$/ZnO core-shell nanowire sensor and **(b)** pure ZnO nanowire sensor for different NO_2 concentrations at 25 °C.

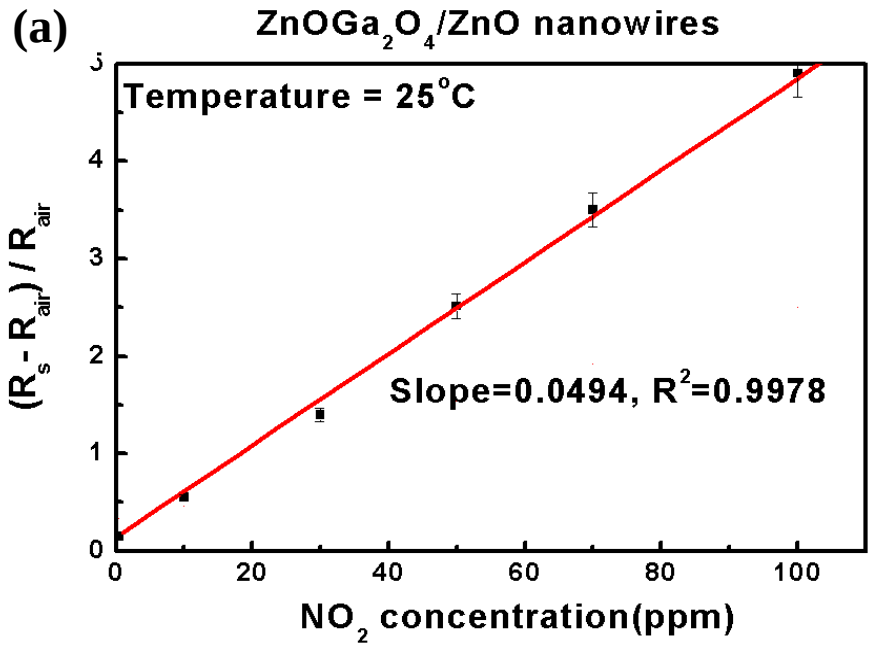

Figure 9. *Cont.*

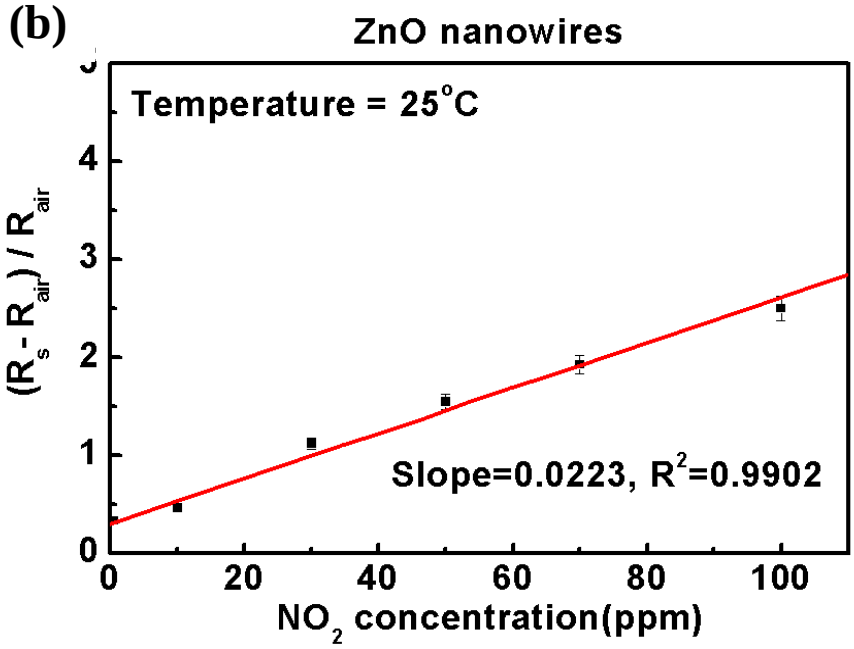

The calculation of slope can be used as an index of sensor sensitivity, and it is obvious that the slope of $ZnGa_2O_4$/ZnO core-shell nanowires is greater than twice that of of the ZnO nanowires. This demonstrates that the sensitivity of NO_2 gas detection by the $ZnGa_2O_4$/ZnO core-shell nanowires can be significantly enhanced at room temperature. Both tests reveal good linear relationships ($R^2 > 0.99$) between sensitivity and gas concentration. The response time to detect 100 ppm NO_2 is about 90 seconds to reach a stable state, and recovery time back to the background is about 120 seconds at room temperature. In contrast, the sensitivity of the $ZnGa_2O_4$/ZnO core-shell nanowires at 250 °C is much greater than that at 25 °C, but the response time is too long to reach stability. The results show that the $ZnGa_2O_4$/ZnO core-shell nanowires based sensors possess the best response and recovery with greater repeatability for NO_2 sensors occurred at room temperature.

All the metal oxide sensors inevitably have the problem of selectivity in practical NO_2 detection applications, especially in the presence of reducing gases, such as H_2, CO, VOCs. Most gases sensors including those for VOCs and EtOH can only work properly at much higher temperatures above 200°C. It is therefore a great demand for NO_2 sensors working effectively at ordinary temperatures so that the interferences can be substantially reduced. At room temperature, the $ZnGa_2O_4$/ZnO core-shell nanowires based sensors as NO_2 sensors present the following characteristics: (1) good linear relationship between sensitivity and NO_2 concentrations, (2) the utmost response (<90 s) and (3) a useful recovery period (<120 s) with greater repeatability for NO_2 detection. In the future work of this study will be extended for improving selective and sensitivity with low-temperature operation. For expansion of its potential application, the further investigation in terms of specificities and sensitivities on other types of gas detection will be conducted in low-temperature settings.

4. Conclusions

This investigation reports on the growth of $ZnGa_2O_4$/ZnO core-shell nanowires on patterned ZnO:Ga/SiO_2/Si templates and the fabrication of the NO_2 gas sensors based on these $ZnGa_2O_4$/ZnO core-shell nanowires. The $ZnGa_2O_4$/ZnO core-shell nanowires grown on a sputtered ZnO:Ga layer were vertically aligned while those grown directly on the SiO_2 layer were randomly oriented, to form the simple sensors with homogenized nanostructure. The $ZnGa_2O_4$/ZnO core-shell nanowires demonstrate good linear relationship between sensitivity and NO_2 concentration both at 250 °C and 25 °C. The NO_2 gas detection of the $ZnGa_2O_4$/ZnO core-shell nanowires sensors present its best response (<90 s) and recovery period (<120 s) with greater repeatability at room temperature. The results indicate that the developed $ZnGa_2O_4$/ZnO core-shell nanowires based sensors are highly promising for industrial applications.

Acknowledgements

This research was funded according to the project "Development of a smart wireless gas sensing SoC for health and environmental applications" (98-EC-17-A-02-S2-0125), which was granted by Ministry of Economic Affairs, Taiwan, R.O.C. The fabrication processes were carried out in the National Nano Device Laboratories and the Center for Micro/Nano Science and Technology (CMNST) at National Cheng Kung University (NCKU). We deeply appreciate the assistance of the respective staffs in this study.

References and Notes

1. Guidotti, T.L. The higher oxides of nitrogen: inhalation toxicology. *Environ. Res.* **1978**, *15*, 443–472.
2. Richters, A.; Kuraitis, K. Inhalation of NO_2 and blood borne cancer cell spread to the lungs. *Arch. Environ. Health* **1981**, *36*, 36–39.
3. Baratto, C.; Sberveglieri, G.; Onischuk, A.; Caruso, B.; di Stasio, S. Low temperature selective NO_2 sensors by nanostructured fibres of ZnO. *Sens. Actuat. B: Chem.* **2004**, *100*, 261–265.
4. Nenov, T.G.; Yordanov, S.P. *Ceramic Sensors-Technology and Applications*; Technomic Publishing: Lancaster, PA, USA, 1996.
5. Meixner, H.; Lampe, U. Metal oxide sensors. *Sens. Actuat. B:Chem.* **1996**, *33*, 198–202.
6. Moseley, P.T. Solid state gas sensors. *Meas. Sci. Technol.* **1997**, *8*, 223–237.
7. Lu, G.; Miura, N.; Yamazoe, N. Stabilized zirconia-based sensors using WO_3 electrode for detection of NO or NO_2. *Sens. Actuat. B: Chem.* **2000**, *65*,125–127.
8. Nakata, S.; Shimanoe, K.; Miura, N.; Yamazoe, N. Field effect transistor type NO_2 sensor combine with $NaNO_2$ auxiliary phase. *Sens. Actuat. B: Chem.* **1999**, *60*, 49–56.
9. Miura, N.; Ono, M.; Shimanoe, K.; Yamazoe, N. A compact solid-state amperometric sensor for detection of NO_2 in ppb range. *Sens. Actuat. B: Chem.* **1998**, *49*, 101–109.
10. Ferro, R.; Rodriguez, J.A.; Bertrand, P. Development and characterization of a sprayed ZnO thin film-based NO_2 sensor, *Phys. Stat. Sol.* (c) **2005**, *10*, 3754–3757.

11. Sergiu, T.; Shishiyanu, T.; Shishiyanu, S.; ; Lupan, O.I. Sensing characteristics of tin-doped ZnO thin films as NO_2 gas sensor. *Sens. Actuat. B: Chem.* **2005**, *107*, 379–386.
12. Steffes, H.; Imawan, C.; Solzbacher, F.; Obermeier, E. Enhancement of NO_2 sensing properties of In_2O_3-based thin film using an Au or Ti surface modification. *Sens. Actuat. B: Chem.* **2001**, *78*, 106–112.
13. Tong, M.; Dai, G.; Wu, Y.; He, X.; Gao, D. WO_3 thin film prepared by PECVD technique and its gas sensing properties to NO_2. *J. Mater. Sci.* **2001**, *36*, 2535–2538.
14. Lee, D.S.; Lim, J.W.; Lee, S.M.; Huh, J.S.; Lee, D.D. Fabrication and characterization of micro-gas sensor for nitrogen oxide gas detection. *Sens. Actuat. B: Chem.* **2000**, *64*, 31–36.
15. Cantalini, C.; Sun, H.T.; Faccio, M.; Pelino, M.; Santucci, S.; Lozzi, L.; Passacantando, M., NO_2 sensitivity of WO_3 thin film obtained by highvacuum thermal evaporation. *Sens. Actuat. B: Chem.* **1996**, *60*, 81–87.
16. Lee, D.S.; Han, S.D.; Lee, S.M.; Huh, J.S.; Lee, D.D. The TiO_2-adding effects in WO_3-based NO_2 sensors prepared by coprecipitation and precipitation method. *Sens. Actuat. B: Chem.* **2000**, *65*, 331–335.
17. Lee, D.S.; Han, S.D.; Huh, J.S.; Lee, D.D. Nitrogen oxides-sensing characteristics of WO_3-based nanocrystalline thick film gas sensor. *Sens. Actuat. B: Chem.* **1999**, *60*, 57–63.
18. Chung, Y.K.; Kim, M.H.; Um, W.S.; Lee, H.S.; Song, J.K.; Choi, S.C.; Yi, K.M.; Lee, M.J.; Chung, K.W. Gas sensing properties of WO_3 thick film for NO_2 gas dependent on process condition. *Sens. Actuat. B: Chem.* **1999**, *60*, 49–56.
19. Giulio, M.D.; Micocci, G.; Serra, A.; Tepore, A. Sputter deposition of tungsten oxide for gas sensing applications. *J. Mater. Sci.* **1998**, *9*, 317–322.
20. Kumar, N.; Dorfman, A.; Hahm, J. Fabrication of optically enhanced ZnO nanorods and microrods using novel biocatalysts. *J. Nanosci. Nanotechnol.* **2005**, *5*, 1915–1918.
21. Hazra, S.K.; Basu, S. Hydrogen sensitivity of ZnO p–n homojunctions. *Sens. Actuat. B: Chem.* **2006**, *117*, 177–182.
22. Wagh, M.S.; Jain, G.H.; Patil, D.R.; Patil, S.A.; Patil, L.A. Modified zinc oxide thick film resistors as NH3 gas sensor. *Sens. Actuat. B: Chem*. **2006**, *115*, 128–133.
23. Wollenstein, J.; Plaza, J.A.; Cane, C.; Min, Y.; Bottner, H.; Tuller, H.L. A novel single chip thin film metal oxide array. *Sens. Actuat. B: Chem*. **2003**, *93*, 350–355.
24. Nakamura, Y.; Zhuang, H.; Kishimoto, A. Enhanced CO and CO_2 gas sensitivity of the CuO/ZnO heterocontact made by quenched CuO ceramics. *J. Electrochem. Soc.* **1998**, *145*, 632–638.
25. Liu, C.Y.; Chen, C.F.; Leu, J.P. Fabrication and CO Sensing Properties of Mesostructured ZnO Gas Sensors. *J. Electrochem. Soc.* **2009**, *156*, J16-J19.
26. Hsueh, T.J.; Chen, Y.W.; Chang, S.J.; Wang, S.F.; Hsu, C.L.; Lin, Y. R.; Lin, T.S.; Chen, I.C. ZnO nanowire-based CO sensors prepared at various temperatures. *J. Electrochem. Soc.* **2007**, *154*, J393–J396.
27. Hsueh, T.J.; Chen, Y.W.; Chang, S.J.; Wang, S.F.; Hsu, C.L.; Lin, Y. R.; Lin, T.S.; Chen, I.C. ZnO nanowire-based CO sensors prepared on patterned ZnO:Ga/SiO2/Si templates. *Sens. Actuat. B: Chem.* **2007**, *125*, 498–503.
28. Hsueh, T.J.; Chang, S.J.; Lin, Y.R.; Chen, I.C.; Hsu, C.L. ZnO nanotube ethanol gas sensor. *J. Electrochem. Soc.* **2008**, *155*, K152–K155.

29. Heo,Y. W.; Varadarajan, V.; Kaufman, M.; Kim, K.; Norton, D.P.; Ren, F.; Fleming, P. H. Site-specific growth of ZnO nanorods using catalysis-driven molecular-beam epitaxy. *Appl. Phys. Lett.* **2002**, *81*, 3046–3048.
30. Wang, J.X.; Sun, X.W.; Yang, Y.; Huang, H.; Lee, Y.C.; Tan, O.K.; Vayssieres, L. Hydrothermally grown oriented ZnO nanorod arrays for gas sensing applications. *Nanotechnol.* **2006**, *17*, 4995–4998.
31. Tseng, Y.K.; Hsu, H.C.; Hsieh, W.F.; Liu, K.S.; Chen, I.C. A Two-step Oxygen Injection Process for Growing ZnO Nanorods. *J. Mater. Res.* **2003**, *18*, 2837–2844.
32. Tseng, Y.K.; Huang, C.J.; Cheng, H.M.; Lin, I.N.; Liu, K.S.; Chen, I.C. Characterization and field emission properties of needle-like zinc oxide nanowhiskers grown vertically on conductive zinc oxide films. *Adv. Funct. Mater.* **2003**, *13*, 811–814.
33. Hsu, C.L.; Chang, S.J.; Hung, H. C.; Lin, Y.R.; Lu, T.H.; Tseng, Y.K.; Chen, I.C. Selective growth of vertical ZnO nanowires on ZnO:Ga/Si_3N_4/SiO_2/Si templates. *J. Vacuum Sci. and Technol. B: Microelectron. Nanometer Struct.* **2005**, *23*, 2292–2296.
34. Hsu, C.L.; Chang, S.J.; Hung, H. C.; Lin, Y.R.; Lu, T.H.; Huang, C.J.; Tseng, Y.K.; Chen, I.C. Vertical single crystal ZnO nanowires grown on ZnO:Ga/glass templates. *IEEE Trans. nanotechnol.* **2005**, *4*, 649–654.
35. Hsu, C.L.; Chang, S.J.; Hung, H.C.; Tseng, Y.K.; Lin, Y.R.; Huang, C.J.; Chen, I.C. Well aligned vertically Al-doped ZnO nanowires synthesized on ZnO:Ga/glass templates". *J. Electrochem. Soc.* **2005**, *152*, G378–G381.
36. Hsu, C.L.; Chang, S.J.; Lin, Y.R.; Tseng, Y.K.; Tsai, S.Y.; Chen, I.C. Vertically well aligned P-doped ZnO nanowires synthesized on ZnO:Ga/glass templates. *Chem. Comm.* **2005**, *28*, 3571–3573.
37. Hsu, C.L.; Lin, Y.R.; Chang, S.J.; Tseng, Y.K.; Tsai, S.Y.; Chen, I.C. Vertical $ZnGa_2O_4$/ZnO nanorods core shell grown on ZnO/glass template by reactive evaporation. *Chem. Phys. Lett.* **2005**, *411*, 221–224.
38. Hsu, C.L.; Lin, Y.R.; Chang, S.J.; Lu, T.H.; Lin, T.S.; Tsai, S.Y.; Chen, I.C. Influence of the formation of the second phase in ZnO/Ga nanowire systems. *J. Electrochem. Soc.* **2006**, *153*, G333–G336.
39. Yang, S.H. Electrophoretic Prepared $ZnGa_2O_4$ Phosphor Film for FED. *J. Electrochem. Soc.* **2003**, *150*, H250–H253.
40. Kang, S.W.; Jeon, B.S.; Yoo, J.S.; Lee, J.D. Optical characteristics of the phosphor screen in field-emission environments. *J. Vac. Sci. Technol. B.* **1997**, *15*, 520–523.
41. Kawazoe, H.; Ueda, K. Transparent conducting oxides based on the spinel structure. *J. Am. Ceram. Soc.* **1999**, *82*, 3330–3336.
42. Lee, Y.E.; Norton, D.P.; Budai, J.D.; Wei, Y. Enhanced ultraviolet photoconductivity in semiconducting $ZnGa_2O_4$ thin films. *J. Appl. Phys*. **2001**, *90*, 3863–3866.
43. Hsueh, T.J.; Chang, S.J.; Lin, Y. R.; Tsai, S.Y.; Chen I.C.; Hsu, C.L. A Novel Method for the Formation of Ladder-like ZnO Nanowires. *Cryst. Growth Des.* **2006**, *6*, 1282–1284.
44. Mitra, P.; Chatterjee, A.P.; Maiti, H.S. ZnO thin film sensor. *Mater. Lett.* **1998**, *35*, 33–38.
45. Kohl, D. The role of noble metals in the chemistry of solid-state gas sensor. *Sens. Actuat. B* **1990**, *1*, 158–165.

46. Sahay, P.P. Zinc oxide thin film gas sensor for detection of acetone. *J. Mater. Sci.* **2005**, *40*, 4383–4385.
47. Belysheva, T.V.; Bogovtseva, L.P.; Kazachkov, E.A.; Serebryakova, N.V. Gas- sensingproperties of doped In_2O_3 films as sensors for NO_2 in air. *J. Anal. Chem.* **2003**, *58*, 583–587.
48. Ferro, R.; Rodriguez, J.A.; Bertrand, P. Peculiarities of nitrogen dioxide detection with sprayed undoped and indium-doped zinc oxide thin films. *Thin Solid Films* **2008**, *516*, 2225–2230.
49. Sadek, A.Z.; Choopun, S.; Wlodarski, W.; Ippolito, S.J.; Kalantar-zadeh, K. Characterization of ZnO nanobelt-based gas sensor for H2, NO_2, and hydrocarbon sensing. *IEEE Sens. J.* **2007**, *7*, 919–924.